European Food Research and Technology (2022) 248:1525–1539
https://doi.org/10.1007/s00217-022-03982-4

ORIGINAL PAPER

Kinetic modeling of a Sangiovese wine's chemical and physical parameters during one-year aging in different tank materials

Lorenzo Guerrini[1] · Francesco Maioli[2] · Monica Picchi[2] · Bruno Zanoni[2] · Alessandro Parenti[2] · Valentina Canuti[2]

Received: 7 December 2021 / Revised: 4 February 2022 / Accepted: 8 February 2022 / Published online: 24 February 2022

Abstract
The present study aimed to model the kinetics of factors involved in wine aging to highlight the effects caused by different tank materials. It is known that materials affect wine composition through releasing of tannins, elementals and allowing different level of oxygen permeation. To monitor how the composition of a red wine was influenced by the contact with different kind of material, a Sangiovese red wine from the 2018 harvest was aged for one-year simultaneously in six different 5 hL tank materials including stainless steel, epoxy-coated concrete, uncoated concrete, raw earthenware, new and used oak wood. The registered differences were described through kinetic modeling of some wine's chemical and physical parameters. In particular, the one-year evolution of the dissolved oxygen, redox potential and phenolic composition of the wines showed significant differences according to the tank material. Like the oak barrels, the raw earthenware amphorae and uncoated concrete tanks enhanced the polymerisation of the phenolic fraction of the wine. Instead, the stainless steel and epoxy-coated concrete proved to be the most chemically inert materials as they showed the least variability of redox potential and the lowest degree of color evolution.

Keywords Dissolved oxygen · Oenological tank materials · Raw earthenware amphora · Redox potential · Uncoated concrete · Wine aging kinetics

Introduction

Aging is a very delicate phase in the red wine production process. Many reactions occur during this phase, and the management of these transformations is always critical. The main changes are caused by the oxidative processes which induce condensation between the free anthocyanins and tannins, allowing the formation of stable polymers [1]. The formation of all these anthocyanin-derived pigments during aging seems to cause the changes observed in wine color, from the initial purple–red hue of young red wines to the brick-red shade characteristic of aged wines. Several factors can co-participate in the formation of the polymeric pigments which promote stabilization of the red wine color over time [2]. These include the phenol composition itself, dissolved oxygen (DO), oxidation–reduction potential (ORP) and the kind of tank material.

It is well known that oxidation and reduction reactions play a key role during wine aging [3], affecting the ORP value of wine. According to the Nernst equation, redox potential depends on both the ratio of the sum of the activities of redox couples in the system, and on the pH value, temperature and dissolved oxygen concentration [4]. Phenolic compounds consume a considerable amount of oxygen by acting as electron acceptors and are responsible for the potentiometric equilibrium of wine [5]. Acetaldehyde is reactive and takes part in several reactions with wine phenolics during aging. One of the most important reactions involves the anthocyanins and flavanols in the formation of methylmethine-bridged compounds and ethyl-linked oligomers [6, 7]; the above compounds can further react with additional acetaldehyde, anthocyanins and flavanols to

✉ Francesco Maioli
francesco.maioli@unifi.it

[1] Department of Land, Environment, Agriculture and Forestry (TeSAF), University of Padua, Viale dell'Università 16, 35020 Legnaro, Padova, Italy

[2] Department of Agricultural, Food, Environmental, and Forestry Sciences and Technologies (DAGRI), University of Florence, Piazzale delle Cascine 18, 50144 Firenze, Italy

generate a pyran ring, or other polymeric-type structures, which can alter the wine sensory attributes [8, 9]. In most of these reactions, oxygen plays a central role. A moderate exposure of wine to air can be beneficial for wine quality; DO in wine can rapidly react with phenolic compounds with an *O*-diphenol function under the catalytic action of a metal such as copper or iron, causing a cascade of chemical transformations [2].

It is essential to monitor ORP, closely related to the DO value, during wine aging to have both an insight into the oxidation and reduction ability of wine [10] and to understand the oxidation–reduction reactions as a function of the different aging tank materials. The measurement of DO provides an indirect index of the oxygen supply during aging: at the point of equilibrium, the concentration of DO is equal to the amount of oxygen transferred into the tank through the material it is made of, minus the amount of oxygen consumed by the wine [11].

Recently, tanks made of different materials have been rediscovered in oenology, but there are only a limited number of technical reports and peer-reviewed papers on monitoring red wine aging in different tank materials, including concrete and earthenware [12]. In addition, no complete experimental designs of all the oenological tank materials are available in the literature.

Some authors [13–15] have investigated the evolution during aging of a white wine in amphorae, stainless steel tanks and oak barrels. They highlighted that different wines can be obtained from a single variety of grape by using different types of containers. Other authors [16] have studied the evolution of DO and ORP during aging of a white wine in both amphorae and stainless steel tanks, showing the impact of tank materials on the chemical and sensory characteristics of wines. In particular, wines aged in raw earthenware amphorae differed in terms of minerality, gustatory–olfactory intensity, structure and harmony. Few authors have compared red wine aging in different tank materials; however, Castellari et al. [17] monitored the composition of red wine during aging in concrete tanks, different sizes of oak barrels and stainless steel tanks, showing significant differences in the levels of DO: it resulted higher in small-volume oak barrels (< 250 L), and similar in concrete and large-volume oak barrels (> 250 L). Other authors [18, 19] made a comparison between red wine aging in oak barrels and alternative systems (stainless steel tanks with staves, chips, oenotannins and micro-oxygenation), while monitoring the DO, ORP and color evolution of the wines. These authors highlighted the importance of monitoring ORP to highlight real-time modifications in wine according to aging modality.

Due to the numerous factors involved in wine evolution during aging, the mathematic modeling of selected parameters could represent a useful tool for understanding and describing the variability of such complex system. In fact, both the complexity and quality of wine are dependent on several intrinsic (wine composition) and extrinsic variables (wine's dissolved oxygen levels, racking operations, storage temperature, and tank materials), that are empirically known to influence the aging process [20]. Moreover, given an initial wine chemical composition, modeling can allow the development of relatively simplified prediction tools to estimate a wine's future condition.

There are numerous studies on modeling phenolic extraction during red wine production [21, 22] and alcoholic fermentation [23, 24]. However, to predict the effect on wine composition and evolution, few kinetic modeling studies have been carried on the wine parameters affecting aging. Martins et al. [25] modeled the DO and temperature in Porto wines during aging, evidencing the interaction effects of the considered parameters on some key wine volatiles. Other authors have modeled the phenolic extraction in oak barrels to describe the mechanism and kinetics of phenolic transfer from wood to wine [26].

The present study aims to model the evolution of Sangiovese red wine during one-year, industrial-scale aging simultaneously in different tank materials (stainless steel, epoxy-coated concrete, uncoated concrete, raw earthenware, new and used oak wood), to describe how the tank material could both allow the mass transfer of different amounts of oxygen and affect the oxidation and reduction reactions in wine.

Materials and methods

Wine treatments and tank materials

The wine used for the experiment was a Sangiovese from the 2018 harvest. After completing the malolactic fermentation, it was centrifuged (0 NTU was set on the nephelometer installed on the centrifuge GEA Westfalia Separator Group GmbH, GSC 60-03-077 and racked in the following tanks: stainless steel tank (SS), epoxy-coated concrete tank (CC), uncoated concrete tank (CR), raw earthenware amphora (AN), new oak barrel (TN) and used oak barrel (TO). The volume of each tank was 5 hL. The new and used oak barrels were made in French oak, medium toasted, from Garbellotto (Sacille, Pordenone, Italy). The used barrel (TO) was 5 years old and the wine was aged inside the barrel for five times.

The basic chemical parameters of the Sangiovese red wine are reported in Table 1. The total sulphites were adjusted to 50 mg/L during racking. Every tank treatment was set up in triplicate.

The raw earthenware amphorae and uncoated concrete tanks were treated before filling according to the company protocols for first-time use.

Table 1 Chemical characteristics of the 2018 Sangiovese wine used for the study

Alcohol content (% v/v)	Residual sugar (g/L)	Titratable acidity (g/L)	Volatile acidity (g/L)	pH	Malic acid (g/L)	Lactic acid (g/L)	Tartaric acid (g/L)	Citric acid (g/L)	Total SO_2 (mg/L)
13.64	2.71	5.33	0.35	3.39	0.16	0.67	2.18	0.20	48

Fig. 1 Picture of the different tanks positioned in the underground cellar

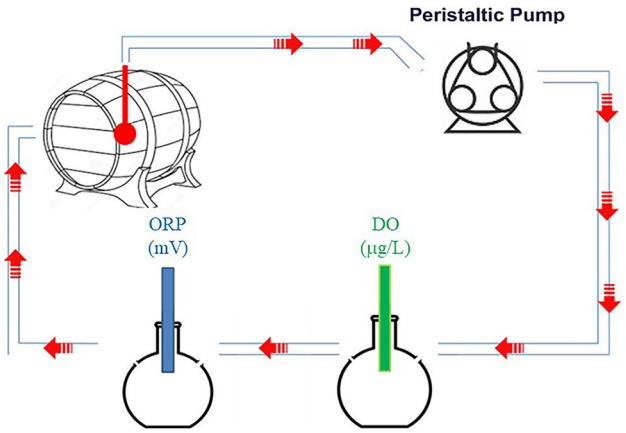

Fig. 2 Recirculation measurement system set up in the cellar to monitor the wine's redox potential (ORP), dissolved oxygen (DO) and temperature (T)

All of the different tanks were placed in an underground cellar at the Cantina Sociale Colli Fiorentini Valvirginio cooperative winery (Montespertoli, Florence, Tuscany), where the temperature ranged between 15 and 22 °C and relative humidity was ~ 80% over the year to simulate real wine aging operating conditions (Fig. 1).

The wines were kept to age simultaneously in the different tanks for 12 months, with no oxygen exposure except for the wine in the SS tanks. In fact, the wine in these tanks was pumped over with air exposure after 6 months of aging, owing to the poor state perceived through sensory analysis.

Samples of the wines aged in the different tank materials were taken for physical and chemical analysis at 0, 4, 10, 17, 24, 31, 50, 63, 124, 156, 191, 219, 240, 262, 293 and 373 days of aging. Particularly, the ORP, DO and temperature (T) values were always measured, while the color parameters and acetaldehyde content were determined from 31 days to the end of aging.

Dissolved oxygen (DO), redox potential (ORP) and temperature (T) measurements

The DO concentration in the wine was measured using an optical oximeter (Oxy Level 2200, Parsec, Italy) and the ORP was monitored using an Edge® pH/ORP meter and an ORP electrode HI36180 (KCl 3.5 M + AgCl, platinum sensor) (Hanna Instrument, Ronchi di Villafranca Padovana, Padova, Italy). The redox potential data were expressed in milli-Volt (mV). Temperature (T) was monitored using the same pH/ORP meter and ORP electrode. Every month after the cleaning process (using a double-junction electrode cleaning solution), the ORP electrode was calibrated with standard redox solutions (purchased from Hanna Instrument) of 468 and 220 mV. All the solutions (calibration, cleaning and storage) were purchased from Hanna Instrument.

To measure the DO and ORP values of the wine inside the different tanks, a closed recirculation system consisting of two glass ampoules and a peristaltic pump was set up. A probe and an electrode were placed in each ampoule to measure, respectively, DO and ORP and the wine was forced to circulate from inside the tank for the time required for probe and electrode stabilization and the measurement (Fig. 2). The electrode took 15 min to obtain a stable measurement, as determined in the preliminary trials, then, following Vivas et al. [27], an additional 15 min was necessary for every DO and ORP measurement. The wine sampling was performed at the same height inside the tanks (50% of the total tank height) each time to avoid differences due to oxygen and redox stratification [4].

Chemical analyses

The standard parameters (pH, titratable acidity, volatile acidity, alcohol content and residual sugars) were measured through FT-IR analyses carried out by means of a FOSS WineScan (FT 120 Reference Manual, Foss, Hamburg, Germany). SO_2 content was measured according to the official EU methods (Regulation (EC) No 479/2008).

The phenolic profile and acetaldehyde content of the wines were investigated according to the literature as follows. Monomeric anthocyanins and polymerised anthocyanins (polymeric pigments) were measured by HPLC [21, 28] and both expressed as malvidin-3-*O*-glucoside (mg/L). The analysis was carried out using a Perkin Elmer Series 200 LC equipped with an autosampler and a diode-array detector (Perkin Elmer, Shelton, CT, USA). Chromatograms were acquired at 520 nm, recorded and processed using Total Chrome Navigator software (Perkin Elmer). Malvidine-3-*O*-glucoside was purchased from Sigma Aldrich (Saint Louis, Missouri, USA).

CIE (Commission Internationale de l'Eclairage) L^*, a^* and b^* color coordinates were also measured according to the literature. Visible spectra were recorded at 400–700 nm reflectance using a Perkin Elmer Lambda 35 UV/Vis spectrophotometer (Perkin Elmer Shelton CT, USA) equipped with the RSA-PE-20 Integrating Sphere accessory assembly (Labsphere, North Sutton, NH, USA). UV WinLab Software was used to record the spectra (version 2.85.04, Perkin Elmer) and CIELab color coordinates were calculated using Colour software (version 3.00, 2001, Perkin Elmer) (D65 illuminant and 10° observer). Color differences between the wines during aging were determined using the ΔE value of the CIELab diagram, according to the following equation (Eq. 1):

$$\Delta E = \sqrt{\left(\Delta L^*\right)^2 + (\Delta a^*)^2 + \left(\Delta b^*\right)^2}. \quad (1)$$

ΔE was calculated as the difference between the wine CIELab coordinates at the time of sampling and the coordinates of the wine at the beginning of the experiment.

Acetaldehyde was determined using an AutoSystem XL gas chromatograph equipped with a flame ionization detector (Perkin Elmer) [29].

All the wine samples were analyzed in triplicate.

Statistics and modeling

All the data collected during the one-year aging were processed to model their evolution, with the tank material (M), storage time (t) and temperature (T) as factors. Stainless steel (SS) was chosen as the reference material. Kinetic models of the collected data were performed as described in the literature when available, otherwise a polynomial curve was adopted to obtain a good phenomenological fit. In the case of polynomial fitting, the tested independent variables were M, t, T and their interactions ($M \times t \times T$). Moreover, t and T were tested at the first, second and third polynomial degree. The variables and interactions were tested for significance with an ANOVA test, and the chosen threshold was $p < 0.05$. According to the principle of model parsimony, all not-significant variables were dropped in the residual and the models were consequently simplified. The Shapiro–Wilk test was used to check the assumption of the normality of the residuals of the models. Once obtained the models, the coefficients for each independent variable used in the model has been reported in the Table 2. Each model has been represented in the Figs. 4, 5, 7, 8, 9, 10, and 11 reporting the value predicted for each material at each sampling time together with its model's standard error term.

The final Principal Component Analysis (PCA) was carried out using all the modeled parameters measured in the wines in the different tanks during one-year aging as a function of t and M.

R software (V. 4.0.0) was used for all the statistical analyses.

Results and discussion

During the wine aging, physical phenomena occurred in relation to the T, DO and ORP measurements. The models describing the changes in DO and ORP as a function of t are reported in Table 2.

Figure 3 shows the wine temperature measured in the different tanks along the one-year aging (dots of the same color represent the replicate treatments). The temperature changed during the one-year aging. At the beginning (in May), the temperature was about 14 °C, increasing to 21 °C during the first 100 days of aging (May–September), decreasing to a minimum of 13 °C at around 300 days (September–March), and increasing again (March–May) following the different seasons of the year (Fig. 3).

Morais et al. [20] previously modeled the DO content in wines using a first-order kinetic and the same equation was used to model the DO values measured in the wine samples ($r = 0.91$) (Eq. 2):

$$\ln [\mathrm{DO}]_{(t)} = \ln [\mathrm{DO}]_0 + k_1 t + k_2 T + k_3 tT + \varepsilon, \quad (2)$$

where k_1, k_2 and k_3 are the coefficients relating to the DO change rate due to t, T and $t \times T$, respectively (Table 2).

The Sangiovese wine samples showed a high amount of DO at the time of racking into the different tanks (Fig. 4), probably due to the centrifugation and the racking itself [30]. The oxygen was quickly consumed by the wines in all the different tanks in the first two weeks of aging (Fig. 4) and the DO values changed significantly according to t, T and $t \times T$ interaction (Table 2). Twenty-four hours after racking, a high amount of DO (roughly 3000 µg/L) was measured. Then, the DO was rapidly consumed by the chemical reactions that occurred in the wines at this stage, reaching values of about 150 µg/L after 18 days. The rate of DO consumption during wine storage, in the interval from saturation to near zero, has previously been described as a pseudo first-order kinetic [31]. A first-order

Table 2 Model equations and significance of all the parameters monitored during the one-year aging in the different tank materials (*M*): redox potential (ORP), dissolved oxygen (DO), acetaldehyde, monomeric anthocyanins, polymeric pigments, CIELab coordinates and ΔE

Variable	M^*	Model equation								Model *r*
		Intercept	T^*	t^*	t^2	t^3	tT	t^2T	t^3T	
DO (0–20 days)	AN	29.23 a	− 1.45	− 2.42 a	ns	ns	0.15	ns	ns	
	CC	29.13 a	− 1.45	− 2.44 a	ns	ns	0.15	ns	ns	
	TO	29.55 a	− 1.45	− 2.44 a	ns	ns	0.15	ns	ns	0.91
	TN	28.39 a	− 1.45	− 2.37 b	ns	ns	0.15	ns	ns	
	CR	29.20 a	− 1,45	− 2.41 a	ns	ns	0.15	ns	ns	
	SS	29.13 a	− 1.45	− 2.44 a	ns	ns	0.15	ns	ns	
ORP	AN	269 a	− 13.4 a	− 0.091 b	ns	ns	ns	ns	5.52	
	CC	219 a	− 11.1 a	− 0.043 a	ns	ns	ns	ns	5.52	
	TO	255 a	− − 12.2 a	− 0.133 b	ns	ns	ns	ns	5.52	
	TN	343 b	− 16.5 b	− 0.177 b	ns	ns	ns	ns	5.52	0.86
	CR	244 a	− 12.1 a	− 0.110 b	ns	ns	ns	ns	5.52	
	SS	226 a	− 11.4 a	− 0.057 a	ns	ns	ns	ns	5.52	
Polymeric pigments (100–230 days)	AN	13.60 b	0.02	0.012	ns	ns	ns	ns	ns	
	CC	13.49 a	0.02	0.012	ns	ns	ns	ns	ns	
	TO	13.46 a	0.02	0.012	ns	ns	ns	ns	ns	
	TN	13.66 b	0.02	0.012	ns	ns	ns	ns	ns	0.92
	CR	13.46 a	0.02	0.012	ns	ns	ns	ns	ns	
	SS	13.40 a	0.02	0.012	ns	ns	ns	ns	ns	
Monomeric anthocyanins (80–250 days)	AN	3.19E+06 a	ns	− 1.27E+04	3.03	ns	ns	0.871	ns	
	CC	3.14E+06 a	ns	− 1.27E+04	3.03	ns	ns	0.871	ns	
	TO	3.47E+06 b	ns	− 1.27E+04	3.03	ns	ns	0.871	ns	
	TN	2.98E+06 a	ns	− 1.27E+04	3.03	ns	ns	0.871	ns	0.89
	CR	3.12E+06 a	ns	− 1.27E+04	3.03	ns	ns	0.871	ns	
	SS	3.07E+06 a	ns	− 1.27+04	3.03	ns	ns	0.871	ns	
Acetaldehyde	AN	2.823 a	ns	ns	5.24E−06	ns	ns	ns	ns	
	CC	2.657 a	ns	ns	5.24E−06	ns	ns	ns	ns	
	TO	3.754 b	ns	ns	5.24E−06	ns	ns	ns	ns	
	TN	1.992 c	ns	ns	5.24E−06	ns	ns	ns	ns	0.39
	CR	2.633 a	ns	ns	5.24E−06	ns	ns	ns	ns	
	SS	2.698 a	ns	ns	5.24E−06	ns	ns	ns	ns	

Table 2 (continued)

Variable	M^*	Model equation								Model r
		Intercept	T^*	t^*	t^2	t^3	tT	t^2T	t^3T	
L*	AN	73.26 a	ns	0.0087	ns	ns	ns	ns	ns	
	CC	73.31 a	ns	0.0087	ns	ns	ns	ns	ns	
	TO	74.05 b	ns	0.0087	ns	ns	ns	ns	ns	
	TN	73.17 a	ns	0.0087	ns	ns	ns	ns	ns	0.62
	CR	73.62 a	ns	0.0087	ns	ns	ns	ns	ns	
	SS	73.07 a	ns	0.0087	ns	ns	ns	ns	ns	
a*	AN	37.6 a	−0.484 a	−0.146 a	4.27E−04	ns	4.95E−03	−1.9E−05	ns	
	CC	36.2 a	−0.360 a	−0.144 a	4.27E−04	ns	4.95E−03	−1.91E−05	ns	
	TO	32.3 b	−0.103 b	−0.138 b	4.27E−04	ns	4.95E−03	−1.91E−05	ns	
	TN	36.2 a	−0.360 a	−0.141 a	4.27E−04	ns	4.95E−03	−1.91E−05	ns	0.96
	CR	37.7 a	−0.452 a	−0.147 a	4.27E−04	ns	4.95E−03	−1.91E−05	ns	
	SS	36.9 a	−0.382 a	−0.144 a	4.27E−04	ns	4.95E−03	−1.91E−05	ns	
b*	AN	0.114 a	ns	0.026 a	−3.64E−05	ns	ns	ns	ns	
	CC	0.845 a	ns	0.026 a	−3.64E−05	ns	ns	ns	ns	
	TO	0.137 a	ns	0.015 b	−3.64E−05	ns	ns	ns	ns	
	TN	0.148 a	ns	0.025 a	−3.64E−05	ns	ns	ns	ns	0.68
	CR	0.970 a	ns	0.024 a	−3.64E−05	ns	ns	ns	ns	
	SS	0.804 a	ns	0.026 a	−3.64E−05	ns	ns	ns	ns	
ΔE	AN	0.35 b	0.13	0.064	−1.10E−04	ns	ns	ns	ns	
	CC	−0.58 a	0.13	0.064	−1.10E−04	ns	ns	ns	ns	
	TO	−1.51 c	0.13	0.064	−1.10E−04	ns	ns	ns	ns	
	TN	−0.35 a	0.13	0.064	−1.10E−04	ns	ns	ns	ns	0.93
	CR	0.04 b	0.13	0.064	−1.10E−04	ns	ns	ns	ns	
	SS	−0.91 a	0.13	0.064	−1.10E−04	ns	ns	ns	ns	

Different letters in the same column indicate statistical significances; *ns* not significant

Correction for the temperature variations, were included in the DO and ORP values

M tank material, *AN* raw earthenware amphora, *CC* coated concrete tank, *TO* used oak barrel, *TN* new oak barrel, *CR* uncoated concrete tank, *SS* stainless steel tank, *T* temperature, *t* time

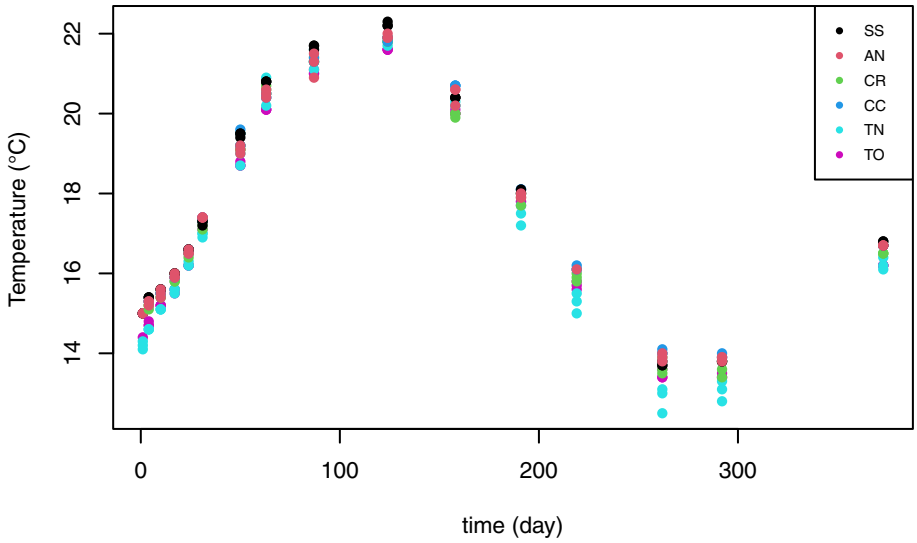

Fig. 3 Evolution of the wine temperature (°C) measured in the different tanks during the one-year aging. Day 0: 7 May; dots of the same color represent the replicate treatments. (*SS* stainless steel tank, *AN* raw earthenware amphora, *CR* uncoated concrete tank, *CC* coated concrete tank, *TN* new oak barrel, *TO* used oak barrel)

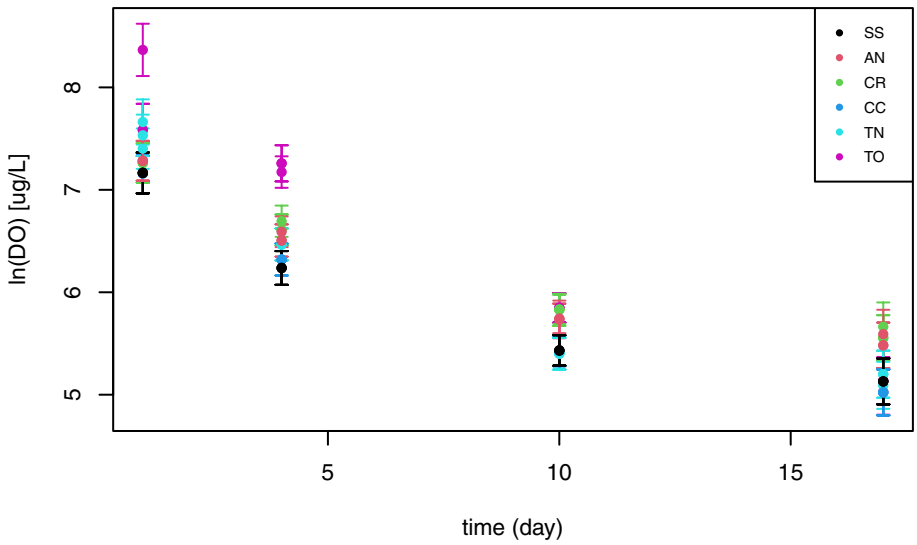

Fig. 4 Kinetic model of the dissolved oxygen (DO—µg/L) in the wine measured in the different tanks during the first 18 days of aging (Error bars represent the standard error; *SS* stainless steel tank, *AN* raw earthenware amphora, *CR* uncoated concrete tank, *CC* coated concrete tank, *TN* new oak barrel, *TO* used oak barrel)

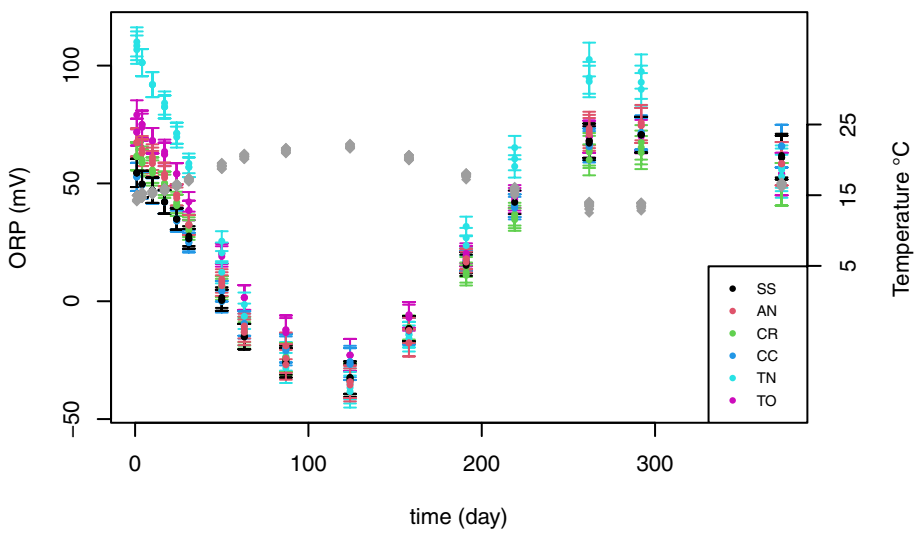

Fig. 5 Kinetic models of the redox potential (ORP—mV) of the wine measured in the different tanks during the one-year aging. The gray diamonds represent the temperature (Error bars represent the standard error; *SS* stainless steel tank, *AN* raw earthenware amphora, *CR* uncoated concrete tank, *CC* coated concrete tank, *TN* new oak barrel, *TO*: used oak barrel)

kinetic describes a concentration-dependent phenomenon: at high DO concentrations the oxygen consumption is fast, while at low concentrations the reaction rate decreases dramatically. In line with the aforementioned literature, the models set up (Table 2) enabled assessment of the rate constant value of the kinetic that depends on (1) wine composition, (2) storage temperature and (3) the effect of the tank material. The initial wine composition was the same for all the treatments and the temperature was considered as covariate in the developed statistical model. Hence, the observed statistically significant difference in the rate constants could be related to the effect of the tanks material.

The wine aged in TN showed significantly slower DO consumption than the wines aged in all the other materials (significant interaction $M \times t$) (Table 2). According to other authors [32], the maximum OTR lasts for approximately the first 20 days and the permeation of oxygen through the oak staves, that reaches a maximum when the barrel is brand new, could account for this difference between the new oak barrels and the other materials.

The DO values did not change significantly between approx. 20 and 150 days of aging, then they increased slightly from 150 to 300 days and decreased between 300 days and one-year (data not shown). According to other authors [20], the above second part of the aging is described according to the same first-order kinetic model mentioned above. However, the model of the second part of the aging had a lower r than the first part ($r=0.65$), and it deviated from linearity at the beginning and at the end of aging; the model only showed linearity in the 150–300-day time range (data not shown).

A certain relationship between the DO values and the ORP experimental values occurred in the wine samples. The ORP showed a continuous decrease in the first 100 days of aging in all the wines aged in the different tanks (Fig. 5), reaching negative values. Then, the ORP rose to 60–100 mV from 120 to 250 days. The rapid decrease at the beginning of aging can be strongly related to the oxygen consumption in all the wine samples. Then the ORP variations were more related to other factors, starting from the temperature. A relationship was found between ORP and T; the highest ORP values were found at the lowest T and vice versa (Fig. 5, Table 2) in agreement with previous studies [5]. These authors highlighted that over a year, the wine temperature during aging in the cellar could be subjected to variations in a range of 5–10 °C; these variations in temperature could affect the redox potential variation in wines in a range of 10–40 mV; so, to standardize the ORP and DO values, a correction factor for the temperature variations was included in the measured values by the instruments.

The ORP variations in the wine aged in the different tanks were similarly modeled by the following polynomial equation ($r=0.86$) (Eq. 3):

$$\mathrm{ORP}_{(t)} = \mathrm{ORP}_0 + k_1 t + k_2 T + k_3 t^3 T + \varepsilon. \quad (3)$$

Six different equations could be written describing the changes in ORP during the wine aging (Table 2). The ANOVA results found no statistically significant differences between the ORP values of the wine aged in epoxy-coated concrete and stainless steel. Concerning the wine in stainless steel, at six months aging (191 days of aging), due to its reductive status at the sensory analysis, it was submitted to a pumping over after the measurements and sampling for the chemical analysis. This practice, applied only to the wine aged in the stainless steel tank, affected the modeling of ORP not more than other factors, given the intrinsic variability of this kind of measurement in wine [18]. Anyway, the r value (0.86) showed a good predictive capability of the model, despite the difficulty of the ORP measurement. The same consideration could be made for the other chemical factors considered and discussed in the next paragraphs. The ORP values of wine aged in raw earthenware amphorae, uncoated concrete tanks and oak barrels showed a different evolution trend. The fastest ORP changes were measured in the wine aged in the oak barrels and raw earthenware amphorae, while the wine in the uncoated concrete tank was the least affected (significant lower coefficient of t). In addition to the effect of temperature changes in the cellar on the ORP values, the differences between the different materials could also be related to oxygen permeation for the raw earthenware amphorae and uncoated concrete tanks [12, 33, 34], and to both oxygen permeation and the release of ellagitannins in the case of the oak barrels [35, 36]. Although polyphenols are the most oxidisable constituents of red wines, they did not contribute to the variation in redox potential [37].

A predictive model of ORP was set up from the DO and T experimental data (Fig. 6). While DO showed a positive coefficient (0.02), the T coefficient was negative (− 11.8). T played a double role; on one hand, in accordance with Henry's law, an increase in T decreased the oxygen solubility in the wine; while, on the other hand, it increased the reaction kinetics. Since the T coefficient was negative, when T increased, ORP decreased. Moreover, DO increased ORP, providing the electron acceptors for the redox reactions that occurred in the wines during aging. In this trial, DO and T could explain 74% of the total variance and they could be considered the main factors in determining ORP. The remaining unexplained variance (26%) could be ascribed to other electron acceptors as well as to measurement errors.

The chemical phenomena related to ORP and DO were monitored by through measurement of the polymeric pigments, monomeric anthocyanins, acetaldehyde and CIELab coordinates during the wine aging.

During the first 100 days of aging, polymerisation between the tannins and anthocyanins occurred slowly and

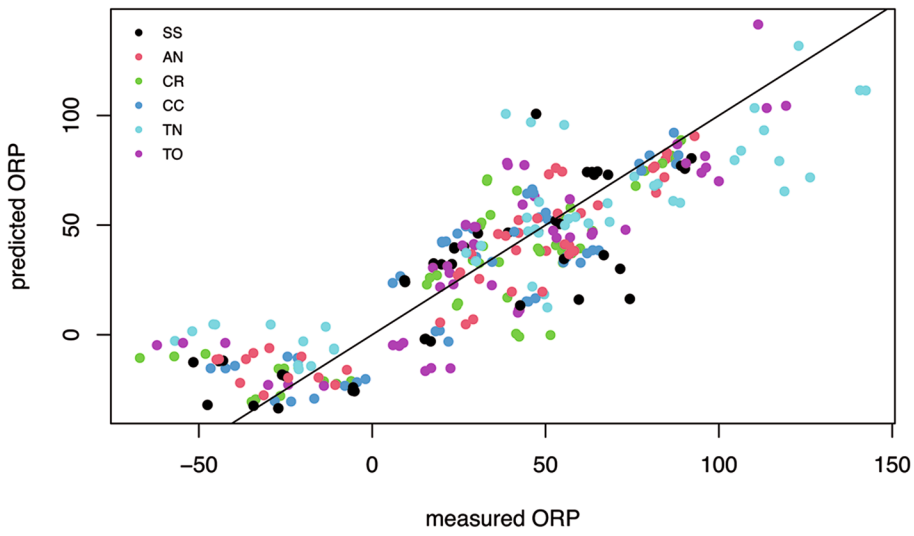

Fig. 6 Prediction model ($r = 0.86$) for redox potential in wines (ORP) using the dissolved oxygen (DO) and temperature (T) measured in wines aged in different tank materials. Dots of the same color represent the treatment replicates

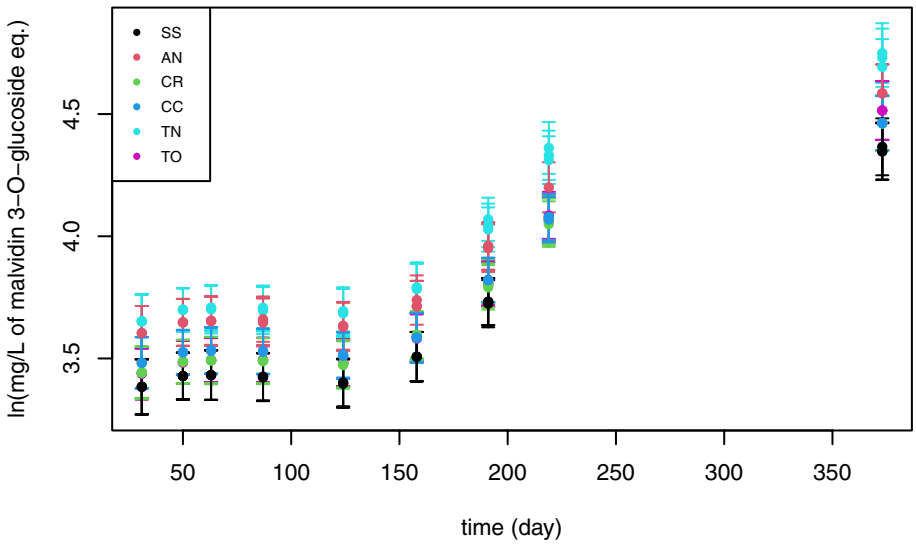

Fig. 7 Kinetic models of the polymeric wine pigments (mg/L of malvidine-3-*O*-glucoside eq.) measured in the different tanks during the one-year aging (Error bars represent the standard error; *SS* stainless steel tank, *AN* raw earthenware amphora, *CR* uncoated concrete tank, *CC* coated concrete tank, *TN* new oak barrel, *TO* used oak barrel)

only a small increase in polymers was seen (Fig. 7). Significant polymerisation occurred instead in all of the wine samples after ~ 150 days; according to some literature studies [32, 36], this highlights the role of DO and ORP parameters in polymerisation between tannins and anthocyanins.

The polymerisation was modeled according to the following equation, which showed a significant different trend for the tank materials ($r = 0.92$) (Eq. 4):

$$\ln\left[\text{polymeric pigments}\right]_{(t)} = \left[\text{polymeric pigments}\right]_0 + k_1 t + k_2 T + \varepsilon, \quad (4)$$

where k_1, k_2 are the coefficients for t and T, respectively (Table 2).

The wine samples aged in the stainless steel tank displayed the slowest formation of polymeric pigments, with no significant differences between the concrete tanks (coated and uncoated) and used oak barrels. The raw earthenware amphorae and the new oak barrel showed the highest polymerisation values. While in the new oak barrel, the higher degree of polymerisation could have been caused by the release of large amounts of both ellagic tannins and oxygen from the oak staves [36, 38, 39], there are not any clear explanation for the raw earthenware amphorae. It could be hypothesized that the raw earthenware amphora releases elementals that could act as a catalyst for polymerization reactions in wines [40]. Moreover, as recently evidenced by other authors [33], the material such earthenware and uncoated concrete showed a clear permeation to oxygen with the exception of epoxy-coated concrete that does not afford any exchanges.

The monomeric anthocyanins content of the wines decreased during aging, with the fastest decrease between 80 and 250 days (Fig. 8). In the literature, the decrease in monomeric anthocyanins has often been related to both

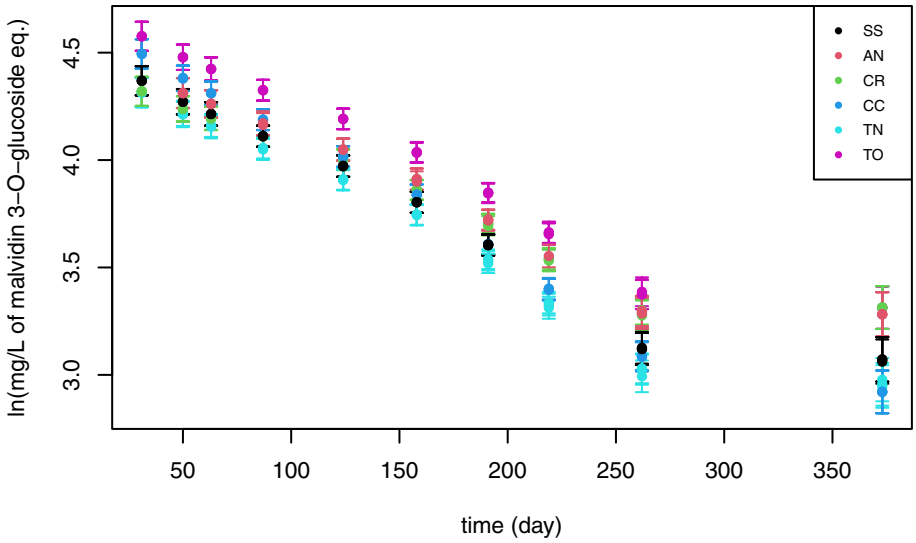

Fig. 8 Kinetic models of the monomeric anthocyanins (mg/L malvidine-3-*O*-glucoside eq.) in the wine measured in the different tanks during the one-year aging (Error bars represent the standard error; *SS* stainless steel tank, *AN* raw earthenware amphora, *CR* uncoated concrete tank, *CC* coated concrete tank, *TN* new oak barrel, *TO* used oak barrel)

oxidation reactions with dissolved oxygen and the formation of polymeric pigments as discussed previously. This decrease, slow during the first three months and then faster [35], could also be consistent with the trends of DO and ORP (Figs. 5 and 6) The above phenomenon was modeled as follows ($r = 0.89$) (Eq. 5):

$$\left[\text{monomeric anthocyanins}\right]_{(t)} = \left[\text{monomeric anthocyanins}\right]_0 + k_1 t + k_2 t^2 + k_3 t^2 T + \varepsilon, \quad (5)$$

where k_1, k_2 and k_3 are the coefficients related to the time (t) at the first, second and third exponents (Table 2). The monomeric anthocyanin content of the wines was higher in the used oak barrel than in all the other materials for the whole duration of the aging, showing significant protective behavior against polyphenol oxidation, probably due to a less permeation of oxygen. However, ellagitannins were still released from the staves, with the slow and continuous formation of polymeric pigments (Fig. 7) [35]. In fact, the age of the barrel could affect the oxygen transmission rate: the older the barrel, the slower the oxygen transmission rate, since most of the wood pores are plugged with wine deposits. Moreover, repeated use of barrel drastically decreases the ellagitannins transferred into wine during aging, owing to the depletion of the oak wood [41].

The formation of polymeric pigments and the decrease in monomeric anthocyanins in the wines was related to the formation of acetaldehyde. This molecule plays a central role during wine aging due to its high reactivity; in particular, the formation of acetaldehyde through ethanol oxidation (following the Fenton reaction) activates the formation of polymeric pigments during wine aging [2]. The acetaldehyde content in the experimental wines remained roughly stable up to 230 days, then it increased (Fig. 9). The following model was set up ($r = 0.39$) (Eq. 6):

$$\left[\text{Acetaldehyde}\right]_{(t)} = \left[\text{Acetaldehyde}\right]_0 + k_1 t^2 + \varepsilon. \quad (6)$$

Despite the low amount of variance explained by the model, it evidenced significant effects of t and M (Table 2). During the aging, when the polymerisation reaction occurred between the anthocyanins and tannins (Fig. 7), the more acetaldehyde was formed, the more acetaldehyde was consumed; therefore, the acetaldehyde content in the wine was able to remain roughly stable. Later, when the polymerization rate decreased, the acetaldehyde content increased. Statistically significant differences were found between the wines aged in the new and used oak barrels; the wine samples aged in used oak barrel showed a higher acetaldehyde content than the other wines, while the wine sample aged in new oak barrel showed the lowest content. The different acetaldehyde content in wines aged in different tank materials could be explained by the polymerisation reaction mediated by this molecule and related to all the characteristics of the tank materials as discussed previously. Condensation reactions mediated by the acetaldehyde in wines contribute to the formation of polymeric pigments when wine is aged in oxidative conditions [2]. It is possible to assume that the wine in the used oak barrel showed the highest acetaldehyde content (Fig. 9) since the formation rate was higher than the rate of consumption due to condensation reactions. Conversely, the wine aged in the new oak barrel could have had the same acetaldehyde formation rate but faster consumption due to the greater release of ellagitannins.

The wine color changed significantly during aging in accordance with the literature data, which have related wine color variation with the polymerisation of anthocyanins and tannins, to form stable colored polymers [8]. The wine lightness (i.e., the L^* CIELab coordinate) increased

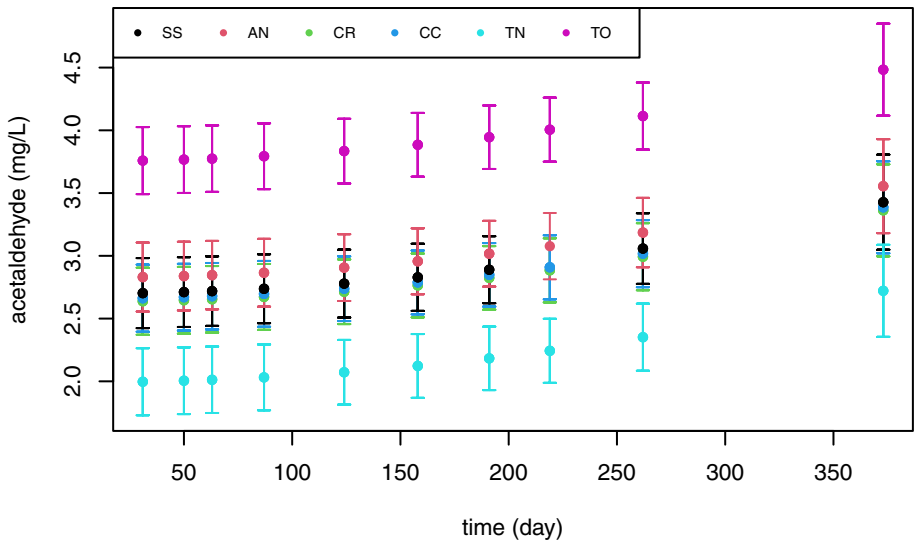

Fig. 9 Kinetic models of the acetaldehyde (mg/L) measured in the wine in the different tanks during the one-year aging (Error bars represent the standard error; *SS* stainless steel tank, *AN* raw earthenware amphora, *CR* uncoated concrete tank, *CC* coated concrete tank, *TN* new oak barrel, *TO* used oak barrel)

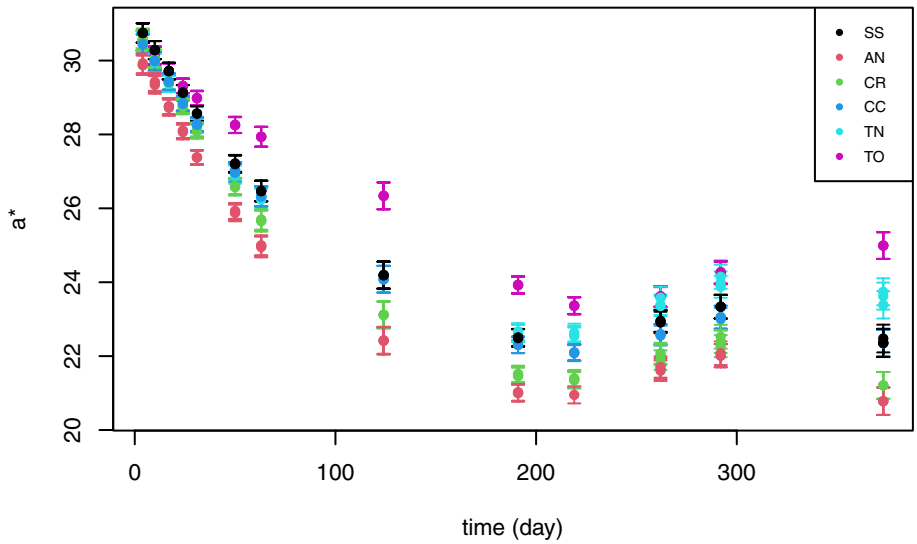

Fig. 10 Kinetic models of a^* CIELab coordinate measured in the wine in the different tanks during the one-year aging (Error bars represent the standard error; *SS* stainless steel tank, *AN* raw earthenware amphora, *CR* uncoated concrete tank, *CC* coated concrete tank, *TN* new oak barrel, *TO* used oak barrel)

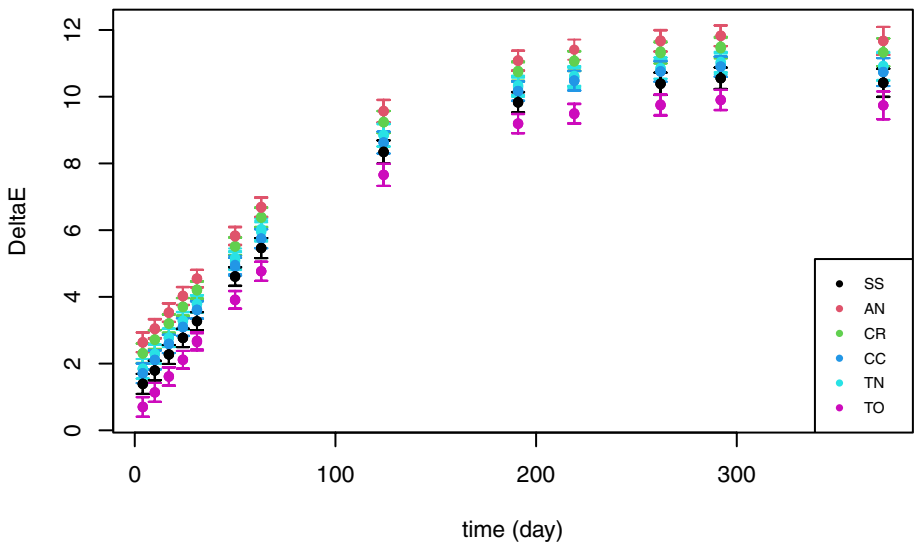

Fig. 11 Kinetic models of the wine ΔE CIELab measured in the different tanks during the one-year aging (Error bars represent the standard error; *SS* stainless steel tank, *AN* raw earthenware amphora, *CR* uncoated concrete tank, *CC* coated concrete tank, *TN* new oak barrel, *TO* used oak barrel)

during aging (Table 2), following a pseudo-zero-order kinetic ($r = 0.62$) (Eq. 7):

$$L^*_{(t)} = L^{|*}_0 + k_1 t + \varepsilon. \quad (7)$$

The lowest L^* values were found in the wine samples aged in the stainless steel tank, whereas the highest were found in the used oak barrel.

The a^* CIELab coordinate values changed significantly during aging as a function of t, T and M, and their interactions (Fig. 10). Between 0 and 100 days a sharp decrease in a^* was measured in all of the wine samples, to then remain roughly stable up to the one-year point. The following kinetic model of the a^* coordinate showed a good fit with the data ($r = 0.96$) (Eq. 8):

$$a^*_{(t)} = a^*_0 + k_1 t + k_2 t^2 + k_3 T + k_4 tT + k_5 t^2 + \varepsilon. \quad (8)$$

The a^* value was only significantly different for the wine aged in the used oak barrel (Table 2), which was less affected by t and T than the other materials. A higher a^* value indicates a more intense red color, consistently with the higher monomeric anthocyanin content of the wine aged in the used oak barrel.

The b^* CIELab coordinate values of the wine increased during aging (Table 2) and were modeled as follows ($r = 0.68$) (Eq. 9):

$$b^*_{(t)} = b^*_0 + k_1 t + k_2 t^2 + \varepsilon. \quad (9)$$

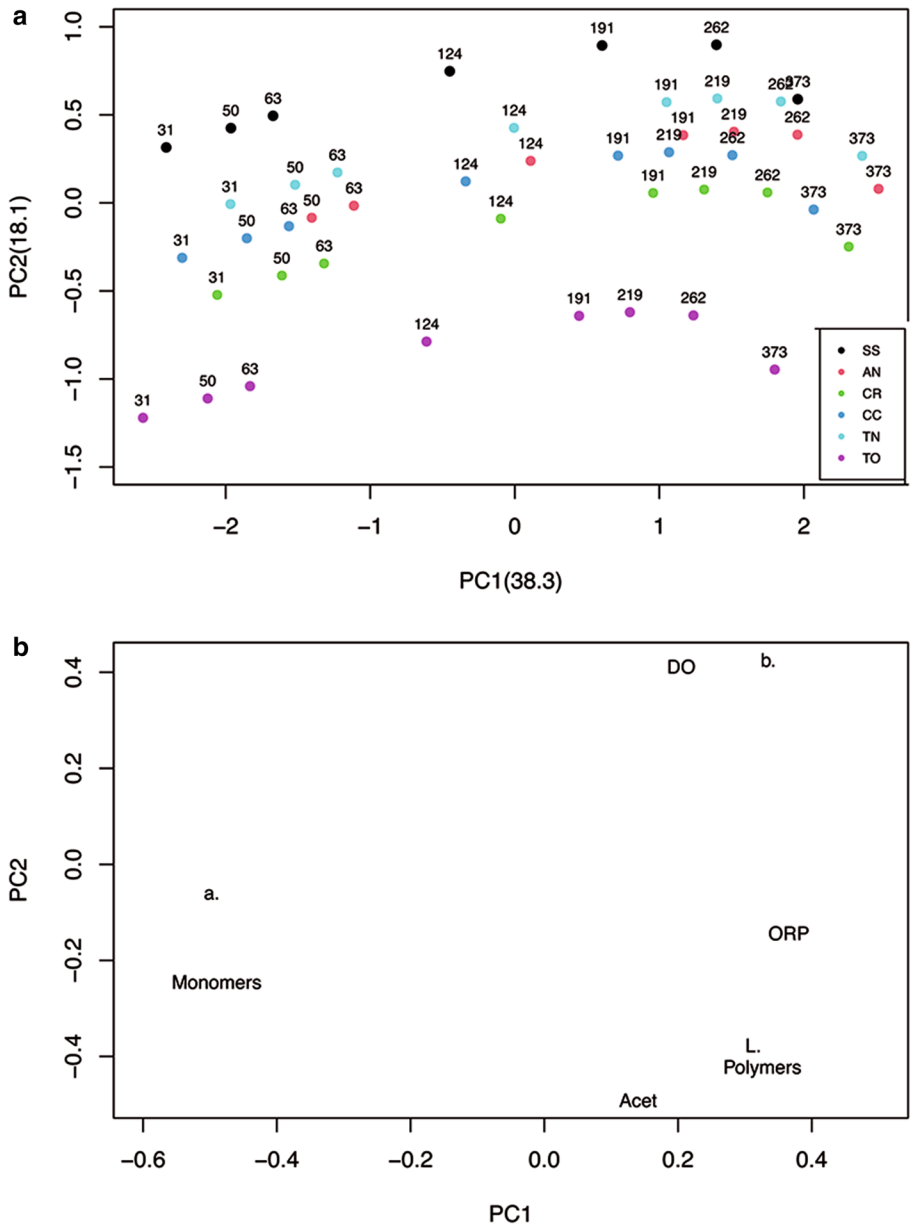

Fig. 12 Principal Component Analysis (PCA) modeled as a function of t and M of the parameters measured in the wines in the different tanks during the one-year aging: (**a**) scores: samples position as a function of the measured parameters at the indicated number of days from the beginning of aging; (**b**) loadings: measured parameters (*SS* stainless steel tank, *AN* raw earthenware amphora, *CR* uncoated concrete tank, *CC* coated concrete tank, *TN* new oak barrel, *TO* used oak barrel)

In terms of the effect of the tank material on the wine characteristics, the only statistically significant differences were related to the wine aged in the used oak barrel (Table 2). In fact, this wine showed a lower increase according to aging time than the other wines.

The color changes were also summarized by the term ΔE. The ΔE values showed an increase with time, reaching an asymptote at ~ 230 days, as a function of T and M (Fig. 11). They were modeled as follows ($r = 0.93$) (Eq. 10):

$$\Delta E_{(t)} = \Delta E_0 + k_1 t + k_2 t^2 + k_3 T + \varepsilon. \quad (10)$$

No significant differences in ΔE were found among the wines in the stainless steel, coated concrete tanks and new oak barrel. The wine samples aged in the raw earthenware amphorae and uncoated concrete tanks had the highest variation in ΔE, whereas the wine samples in the used oak barrel had a significantly lower variation in ΔE than the other wine samples.

At the end, a Principal Component Analysis (PCA) was run to report a global graphical overview of the evolution of all the wine samples during one-year aging in the different tank materials according to all the measured parameters. The PCA scores obtained were also modeled as a function of the variables t and M.

The model results for PC1 and PC2 are reported in Fig. 12. The explained variance was 56.4% and a good separation was evidenced between the wine samples aged in the different tank materials and time. The time sampling (expressed in the same figure as the day of sampling) was distributed along the PC1, indicating that there were differences in the evolution of the wine during aging. At the beginning of aging, the wines were located on the left side of the plot and featured the highest values of monomeric anthocyanins and a^*. During aging, the wine samples evolved as evidenced by the increase in acetaldehyde, polymeric pigments, L^* and b^*, and their positions moved towards the right side of the plot. The distribution of the wines along the PC1 highlighted slow changes in the wine composition during the first 60 days, then the changes accelerated between days 63 and 191, and finally they slowed down again. Among the materials, the wines aged in the raw earthenware amphorae and new oak barrel were found to be significantly different from wine aged in the stainless steel tank in terms of PC1 scores, since they showed a faster movement from the left to the right side of the score plot.

PC2 separated the wine samples according to the different materials. Significant differences were found for the uncoated concrete and coated concrete tanks, and used oak barrel. Despite a similar evolution trend among the wines, their distribution along the PC2 highlighted the influence of the tank material from the 31st day on, and these differences remained stable until the end of monitoring.

These trends translated into a different final composition and kinetic of the wine evolution, highlighting the importance of the kind of tank material.

Conclusions

This study highlighted the redox phenomena tendencies occurring in red wines during one-year aging in tanks of different materials. These tendencies were related to a series of operating conditions and chemical-physical phenomena such as: (1) the oxygenation level of the wines at the beginning of aging; (2) the level of oxygen permeability and impregnation of the tank materials; (3) the amounts of molecules released by the tanks; (4) the wine temperature; and (5) the oxygen consumption rate caused by the different components in the wines. For all the different tank materials, the synergic or antagonistic action of the aforementioned operating conditions and chemical–physical phenomena resulted in a common trend of the physical and chemical parameters relating to the redox state of the wines. In the first approximatively 100 days of aging there was a rapid consumption of oxygen (i.e., decrease in DO) and a rapid decrease in the redox potential, which could be correlated to reactions with rapid oxygen consumption such as the oxidation of polyphenols. From ~ day 150 up to the end of aging, the oxygen level increased slightly, while the redox potential increased, reaching a similar value to the beginning of aging. Rapid oxygen consumption reactions were replaced by slow oxygen consumption (i.e., anthocyanin–tannin ethylene bridge polymerisation reactions), which, as well as the wine temperature, were probably responsible for increasing the redox potential. In the wines, the polymerisation reaction mediated by acetaldehyde seemed to be activated when the redox potential increased, again after reaching the lowest level during the one-year aging, demonstrating that a defined level of redox potential is needed to trigger the reaction. Moreover, all the reactions that occurred in the wines during aging caused a general trend of variation in the wine color, which was similar for all the tanks.

The experimental data were modeled and the kinetic models were able to describe the differences between the wine samples aged in the different tank materials. The stainless steel and epoxy-coated concrete tanks were the least suited to allowing a variation in the redox state of the wines, which was exactly the opposite of the oak barrels; the behavior of the raw earthenware amphorae and uncoated concrete tanks, on the other hand, was somewhere in-between, but tended to be more similar to the oak barrels. The level of oxygen permeability and impregnation of the tanks and the degree of substances released by the tank materials could

explain the well-known greater redox attitude of oak barrels compared to stainless steel and epoxy-coated concrete tanks, which were the most chemically inert. The behavior of the raw earthenware amphorae and the uncoated concrete tanks appears interesting and deserves specific studies to investigate all the above-mentioned phenomena in relation to the chemical composition and production process of the materials.

To conclude, knowledge of the tank characteristics could be considered a useful tool to characterize the wine according to the winery needs.

Acknowledgements Warm thanks go to the Cantina Sociale Colli Fiorentini Valvirginio in Montespertoli (Florence) for allowing us to set up our experiment in its cellar and the support of the company oenologists Marco Puleo and Riccardo Pagliai; to CLC s.r.l. (Carmignano di Brenta, Padova) for providing the concrete tanks; Artenova s.r.l. (Impruneta, Florence) and oenologist Francesco Bartoletti for providing the raw earthenware amphorae.

Declarations

Conflict of interest All of the authors have read the manuscript and affirm that the content of this manuscript has not been published or submitted elsewhere.

Compliance with ethics requirements This article does not contain any studies with human participants or animals performed by any of the authors.

References

1. Glories Y (1990) Oxygène et élevage en barriques. Revue Française D'Œnologie 30(124):91–96
2. Waterhouse AL, Laurie VF (2006) Oxidation of wine phenolics: a critical evaluation and hypotheses. Am J Enol Vitic 57(3):306–313
3. Tomlinson JW, Kilmartin PA (1997) Measurement of the redox potential of wine. J Appl Electrochem 27(10):1125–1134
4. Berovič M, Nemanič J (2019) The role of redox potential measurement in oak barrel wine maturation. Chem Biochem Eng Q 33:153–160. https://doi.org/10.15255/CABEQ.2018.1469
5. Vivas N, Zamora F, Glories Y (1992) Etude des phénomènes d'oxydoréduction dans les vins. Mise au point d'une méthode rapide de mesure du potentiel d'oxydoréduction. OENO One 26(4):271–285. https://doi.org/10.20870/oeno-one.1992.26.4.1191
6. Schmidtke LM, Clark AC, Scollary GR (2011) Micro-oxygenation of red wine: techniques, applications, and outcomes. Crit Rev Food Sci Nutr 51:115–131. https://doi.org/10.1080/10408390903434548
7. Timberlake CF, Bridle P (1976) Interactions between anthocyanins, phenolic compounds, and acetaldehyde and their significance in red wines. Am J Enol Vitic 27:97–105
8. Es-Safi NE, Fulcrand H, Cheynier V, Moutounet M (1999) Competition between (+)-catechin and (−)-epicatechin in acetaldehyde-induced polymerization of flavanols. J Agric Food Chem 47(5):2088–2095. https://doi.org/10.1021/jf980628h
9. He F, Liang NN, Mu L, Pan QH, Wang J, Reeves MJ, Duan CQ (2012) Anthocyanins and their variation in red wines I. Monomeric anthocyanins and their colour expression. Molecules 17(2):1571. https://doi.org/10.3390/molecules17021571
10. Kukec A, Berovič M, Čelan Š, Wondra M (2002) The role of online redox potential measurement in Sauvignon blanc fermentation. Food Technol Biotechnol 40(1):49–55
11. Roussey C, Colin J, du Cros RT, Casalinho J, Perré P (2021) In-situ monitoring of wine volume, barrel mass, ullage pressure and dissolved oxygen for a better understanding of wine-barrel-cellar interactions. J Food Eng 291:110–233. https://doi.org/10.1016/j.jfoodeng.2020.110233
12. Maioli F, Picchi M, Guerrini L, Parenti A, Domizio P, Andrenelli L, Zanoni B, Canuti V (2022) Monitoring of Sangiovese red wine chemical and sensory parameters along one-year aging in different tank materials and glass bottle. ACS Food Sci Technol 2(2):221–239. https://doi.org/10.1021/acsfoodscitech.1c00329
13. Baiano A, Varva G, De Gianni A, Viggiani I, Terracone C, Del Nobile MA (2014) Influence of type of amphora on physicochemical properties and antioxidant capacity of 'Falanghina'white wines. Food Chem 146:226–233. https://doi.org/10.1016/j.foodchem.2013.09.069
14. Martins N, Garcia R, Mendes D, Freitas AMC, da Silva MG, Cabrita MJ (2018) An ancient winemaking technology: exploring the volatile composition of amphora wines. LWT 96:288–295. https://doi.org/10.1016/j.lwt.2018.05.048
15. Rossetti F, Merkyte V, Longo E, Pavlic B, Jourdes M, Teissedre PL, Boselli E (2018) Volatile, phenolic, and sensory profiles of in-amphorae Chardonnay wine by mass spectrometry and chemometric analysis. J Mass Spectrom 53:833–841. https://doi.org/10.1002/jms.4262
16. Baiano A, Varva G (2019) Evolution of physico-chemical and sensory characteristics of Minutolo white wines during aging in amphorae: a comparison with stainless steel tanks. LWT 103:78–87. https://doi.org/10.1016/j.lwt.2018.12.065
17. Castellari M, Simonato B, Tornielli GB, Spinelli P, Ferrarini R (2004) Effects of different enological treatments on dissolved oxygen in wines. Ital J Food Sci 16(3):387–397
18. del Alamo M, Nevares I, Carcel LM (2006) Redox potential evolution during red wine aging in alternative systems. Anal Chim Acta 563:223–228. https://doi.org/10.1016/j.aca.2005.11.017
19. Oberholster A, Elmendorf BL, Lerno LA, King ES, Heymann H, Brenneman CE, Boulton RB (2015) Barrel maturation, oak alternatives and micro-oxygenation: influence on red wine aging and quality. Food Chem 173:1250–1258. https://doi.org/10.1016/j.foodchem.2014.10.043
20. Morais R, Peres E, Boaventura-Cunha J, Mendes J, Cosme F, Nunes FM (2018) Distributed monitoring system for precision enology of the Tawny Port wine aging process. Comput Electron Agric 145:92–104. https://doi.org/10.1016/j.compag.2017.12.019
21. Zanoni B, Siliani S, Canuti V, Rosi I, Bertuccioli M (2010) A kinetic study on extraction and transformation phenomena of phenolic compounds during red wine fermentation. Int J Food Sci Technol 45(10):2080–2088. https://doi.org/10.1111/j.1365-2621.2010.02374.x

22. Cerda-Drago TG, Agosin E, Pérez-Correa JR (2016) Modelling the oxygen dissolution rate during oenological fermentation. Biochem Eng J 106:97–106. https://doi.org/10.1016/j.bej.2015.10.014
23. Colombié S, Malherbe S, Sablayrolles JM (2005) Modeling alcoholic fermentation in enological conditions: feasibility and interest. Am J Enol Vitic 56:238–245
24. Dijken JP, Weusthuis RA, Pronk JT (1993) Kinetics of growth and sugar consumption in yeasts. Antonie Van Leeuwenhoek 63(3–4):343–352
25. Martins RC, Monforte AR, Silva Ferreira A (2013) Port wine oxidation management: a multiparametric kinetic approach. J Agric Food Chem 61(22):5371–5379. https://doi.org/10.1021/jf4005109
26. Kadim D, Mannheim CH (1999) Kinetics of phenolic extraction during aging of model wine solution and white wine in oak barrels. Am J Enol Vitic 50(1):33–39
27. Vivas N, Glories Y, Bertrand A, Zamora F (1996) Principe et méthode de mesure du potentiel d'oxydoréduction dans les vins. Bulletin OIV 69:617–633
28. Peng Z, Iland PG, Oberholster A, Sefton MA, Waters EJ (2002) Analysis of pigmented polymers in red wine by reverse phase HPLC. Aust J Grape Wine Res 8:70–75. https://doi.org/10.1111/j.1755-0238.2002.tb00213.x
29. Bertuccioli M (1982) Direct gas chromatographic determination of some volatile compounds in wine. Vini d'Italia 138:149–156
30. Calderón JF, del Alamo-Sanza M, Nevares I, Laurie F (2014) The influence of selected winemaking equipment and operations on the concentration of dissolved oxygen in wines. Int J Agric Nat Resour 41:273–280. https://doi.org/10.4067/s0718-16202014000200014
31. Ferreira V, Carrascon V, Bueno M, Ugliano M, Fernandez-Zurbano P (2015) Oxygen consumption by red wines. Part I: consumption rates, relationship with chemical composition, and role of SO_2. J Agric Food Chem 63:10928–10937. https://doi.org/10.1021/acs.jafc.5b02988
32. del Alamo-Sanza M, Cárcel LM, Nevares I (2017) Characterization of the oxygen transmission rate of oak wood species used in cooperage. J Agric Food Chem 65:648–655
33. Nevares I, del Alamo-Sanza M (2021) Characterization of the oxygen transmission rate of new-ancient natural materials for wine maturation containers. Foods 10(1):140
34. Baiano A, Mentana A, Quinto M, Centonze D, Longobardi F, Ventrella A, Agostiano A, Varva G, De Gianni A, Terracone C, Del Nobile MA (2015) The effect of in-amphorae aging on oenological parameters, phenolic profile and volatile composition of Minutolo white wine. Food Res Int 74:294–305. https://doi.org/10.1016/j.foodres.2015.04.036
35. Cano-Lòpez M, Lòpez-Roca JM, Pardo-Minguez F, Gòmez Plaza E (2010) Oak barrel maturation vs. micro-oxygenation: effect on the formation of anthocyanin-derived pigments and wine colour. Food Chem 119:191–195. https://doi.org/10.1016/j.foodchem.2009.06.018
36. Martínez-Gil A, Del Alamo-Sanza M, Nevares I (2022) Evolution of red wine in oak barrels with different oxygen transmission rates. Phenolic compounds and colour. LWT 158:113133
37. Danilewicz JC (2012) Review of oxidative processes in wine and value of reduction potentials in enology. Am J Enol Vitic 63:1–10. https://doi.org/10.5344/ajev.2011.11046
38. Liu Y, Zhang XK, Shi Y, Duan CQ, He F (2019) Reaction kinetics of the acetaldehyde-mediated condensation between (−)-epicatechin and anthocyanins and their effects on the colour in model wine solutions. Food Chem 283(17):315–323. https://doi.org/10.1016/j.foodchem.2018.12.135
39. Vivas N, Glories Y (1996) Role of oak wood ellagitannins in the oxidation process of red wines during aging. Am J Enol Vitic 47(1):103–107
40. Cortiella MG, Ubeda C, Covarrubias JI, Laurie VF, Peña-Neira Á (2021) Chemical and physical implications of the use of alternative vessels to oak barrels during the production of white wines. Molecules 26(3):554
41. Navarro M, Kountoudakis N, Gómez-Alonso S, García-Romero E, Canals JM, Hermosín-Gutíerrez I, Zamora F (2016) Comparison between the contribution of ellagitannins of new oak barrels and one-year-used barrels. BIO Web Conf 7:02016. https://doi.org/10.1051/bioconf/20160702016